Photon Hopping and Nanowire Based Hybrid Plasmonic Ring-resonator

Zhiyuan Gu[1], **Shumin Xiao**[2], **Shuai Liu**[1], **Shang Sun**[2], **Kaiyang Wang**[1], **and Qinghai Song**[1,3]

[1]Department of Electrical and Information Engineering
Harbin Institute of Technology, Shenzhen, Guangdong 518055, China
[2]Department of Materials Science and Engineering
Harbin Institute of Technology, Shenzhen, Guangdong 518055, China
[3]National Key Laboratory on Tunable Laser Technology
Harbin Institute of Technology, Harbin 158001, China

Abstract— Here we demonstrate the transmission of waves through a gap in hybrid plasmonic waveguide, which is termed as "photon hopping". Based on the photon hopping, we explore the possibility to achieve high Q resonator by nano-manipulating the nanowire to a pseudo-ring. Our numerical results show that the Q factors, effective mode volumes, and Purcell factors of nanowire based ring-resonator are very close to a perfect hybrid plasmonic ring resonator, expanding the potential applications of nanowires to nano-cavity quantum electrodynamics (QED) and nanolasers.

1. INTRODUCTION

Manipulation of light in subwavelength and nanoscale structures is of central importance for the researches on miniaturizations of coherent light sources and highly integrated photonic network [1]. A number of nanostructures such as nanoparticles [2] and antennas [3] have been successfully developed to control the light confinement and emission in nanoscale. Nanowires are prominent examples due to their intrinsic advantages, e.g., dislocation free single crystalline, cost-effective synthesis, high index of refraction, and broad range of materials [4–6]. In past decade, coherent light sources with tiny effective mode areas have been successfully detected from different nanocavities, including ZnS [7], CdS [8], GaN [9], and GaSb [10] nanowires. However, the performances of such devices face severe challenge when their sizes are further reduced to nanoscale. This is caused by two main limitations. The mode volumes are usually comparable to nanowire dimensions [11]. And the light confinements are very poor due to their extremely low end-facet reflections [12, 13].

Owing to the better confinement of surface plasmon polaritons (SPP) [14], the combination of semiconductor nanowire and plasmonic waveguide has been utilized to reduce the effective mode volume (V_{eff}) [15]. However, the light confinement is still an awesome task for the nanowire based plasmonic devices. Here we demonstrate the photon hopping phenomenon in hybrid plasmonic waveguide and explore its applications in high-Q nanocavities.

2. RESULTS

As depicted in Fig. 1(a), the hybrid waveguide consists of a dielectric nanowire separated from a silver layer by a nanoscale insulating layer with lower refractive index. Here we set $d = 100\,\text{nm}$, $h = 5\,\text{nm}$, $\varepsilon_c = 5.76$ (for CdSe or GaN), and $\varepsilon_d = 1.96$ (for MgF_2). The permittivity of silver is defined with a Drude model. And the material dispersion and loss of dielectric structures are neglected.

The calculated n_{eff} for the hybrid plasmonic mode at 530 nm is only about 1.7, which is not too much higher than the surrounding medium. From the Fresnel law, we can find that the reflectance is only $\sim$ 9% in a wide frequency range, consistent with the small n_{eff}. For the conventional Fabry-Perot like nanowire cavities, their quality (Q) factors can be estimated with the equation $Q = -Lk_a/\ln|r_1r_2|$, where L, k_a, r_1, and r_2 are the nanowire length, propagation constant, and reflection coefficients at two end facets. Following the results in Fig. 1(b), the Q factor of a hybrid plasmonic waveguide with $L = 1\,\mu\text{m}$ is only around 7.5, which prevents short nanowires from lasing and restricts the lower limit of nanowire dimensions.

As the reflection and propagation loss are both low in the hybrid plasmonic waveguide [16–18], most of the waves shall transmit refractively at the end facet. The opened squares in Fig. 1(b) show the calculated transmission spectrum at interface $S1$, where almost 40%–50% of energy can be detected outside the hybrid plasmonic waveguide.

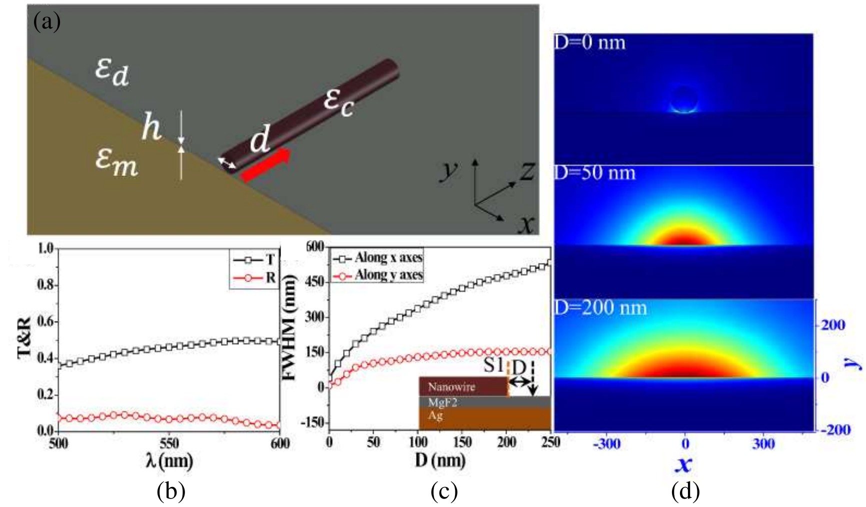

Figure 1: (a) The schematic picture of the hybrid plasmonic waveguide. A semi-infinite long nanowire is placed on a metal substrate insulated by a thin low-index dielectric layer. The end-facet is marked as $S1$. The silver is modeled by Drude model and the permittivity of CdS and MgF_2 are set as $\varepsilon_c = 5.76$ and $\varepsilon_d = 1.96$. (b) The transmission (T, open squares) and reflection (R, open circles) of the waveguide at interface $S1$. Here $d = 100$ nm and $h = 5$ nm. (c) The evolutions of FWHM of the output beam in horizontal direction (open squares) and vertical direction (open circles). (d) The field pattern of propagating mode at the plane with distance $D = 0$, 50, and 200 nm from the interface $S1$.

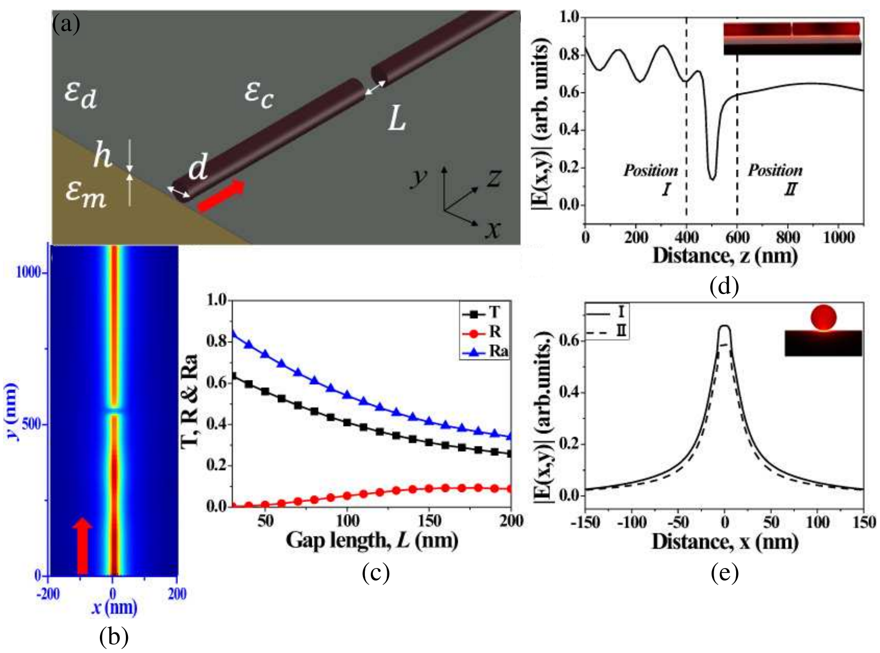

Figure 2: (a) The Schematic picture of two nanowire based hybrid plasmonic waveguide. The separation distance between two nanowires is L. (b) the electric density distribution in MgF_2 insulating layer. Efficient photon hopping can be directly observed. (c) The transmittance (T, black squares), reflectance (R, red dots), and ratio (blue triangles) as a function of L. (d) the electric field along the z-axis. (e) The electric field along x-axis at position I (solid line) and II (dashed line) marked in (d). The insets are the corresponding field patterns.

To explore the possibility of nanoscale light collection, we have studied the field distributions of the transmitted light. With the increasing of distance from end-facet $S1$ (D), we can see that the full width half maximum (FWHM) of the output beam increases gradually from 40 nm at $D = 0$ nm to about 530 nm at $D = 250$ nm in the plane. This divergence is caused by the diffraction of waves from the small aperture, similar to the emission from conventional waveguide. The field distribution in the vertical direction is quite different. While the FWHM also increases at the beginning, it turns to be saturate at $D > 30\,\text{nm}$. From the field distributions in Fig. 1(d), we thus know that the electromagnetic waves transit from hybrid plasmonic mode to regular SPP along the Silver-MgF_2 interface when they leave the hybrid waveguide.

To fully explore the applications of nanowire, we place a nanowire behind the first one. The schematic picture is depicted in Fig. 2(a). Fig. 2(b) shows the electric density distribution of hybrid plasmonic mode at $\lambda = 550\,\text{nm}$ at the Ag-MgF_2 interface. While a gap appears, we can see that the waves mostly transmit into the second nanowire. It is worth to note that the low transmittance doesn't mean the high loss caused by the gap. There is still reflection caused by the interfaces at the gap. The calculated values are shown as red dots in Fig. 2(c). The blue triangles represent the ratio $[Ra = (T + R)/T_{\text{WO}}]$, where T_{WO} is the transmittance in single nanowire with the same overall length without gap. We can see that ratio can be larger than 40% when the separation distance $L < 150\,\text{nm}$, clearly demonstrating the high collecting efficiency of the second waveguide. In principle, the high transmittance is not surprising. Similar to the previous study on the propagation of SPP across narrow grooves in silver film [19], the transmitted waves experience a transition from hybrid plasmonic to regular SPP and a transition back to hybrid plasmonic. Fig. 2(d) shows the field distribution along the z-axis. The reduction of $|E(x, y)|$ at the gap is consistent with the transition processes. Meanwhile, the field distributions before and behind the gap [see Figs. 2(b) and 2(e)] are almost the same, indicating that the transmitted waves follows the same hybrid plasmonic mode as the incident one. Below, we term this process as "photon hopping".

Placing two nanowires end by end is of course possible in nano-manipulation [11]. However, it is extremely difficult to arrange their axles in a single line experimentally as Fig. 2. To explore the light collection for real applications, we have numerically studied the dependences of transmittance on the transverse shift along x-axis (see Fig. 3(a)). The results are summarized in Fig. 3(c). With the increasing of w, the transmittance decreases slowly. When $w = 100\,\text{nm}$ and $d = 50\,\text{nm}$, the transmittance is still around 32%. Taking account the reflection, the ratio Ra is almost 42.5%, which means that almost half energy can be collected by placing two nanowires end by end with slight overlap. The high transmission at large w is consistent with the horizontal divergence of regular SPP in Fig. 1(c). Similarly, the transmittance T and ratio Ra are also quite robust to the tilt of the second wire. When the tilt angle $\theta \leq 40$ degree, the transmittance is higher than 39.5% and the ratio Ra is larger than 49.5%. The examples of field patterns in MgF_2 layer are plotted in Figs. 3(b) and 3(e).

Based on this effect of "photo hopping", we can propose a new scheme to achieve the high

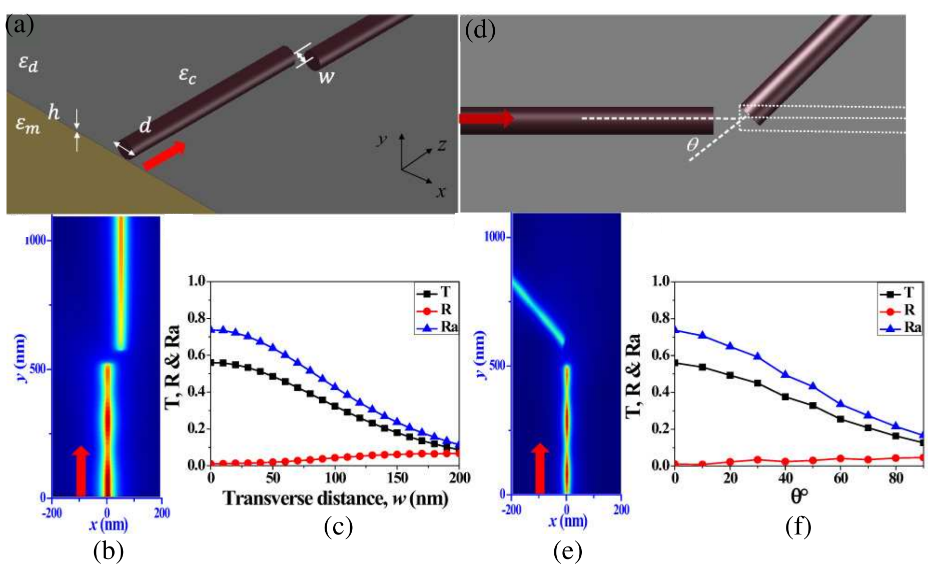

Figure 3: The robustness of the light collection by the second nanowire. (a) and (c) depict the transverse shift and tilt angle. (c) and (f) are the dependence of T, R, and Ra on w and θ, respectively. (b) and (e) show the example electric density distributions with $w = 50\,\text{nm}$ and $\theta = 50$ degree.

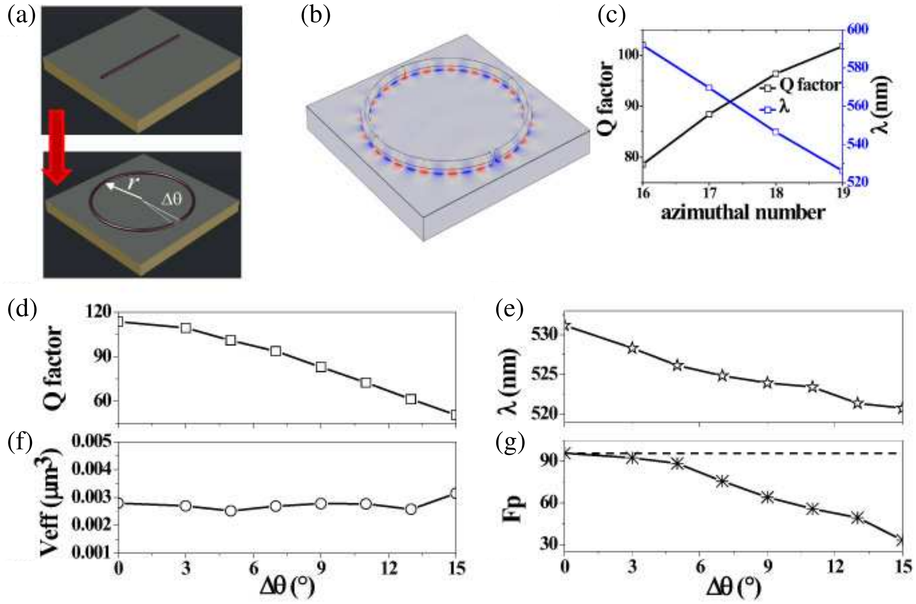

Figure 4: (a) Schematic of hybrid plasmonic ring-resonator. The size parameters of ring resonator and nanowire are $r = 1000\,\text{nm}$ and $d = 100\,\text{nm}$, respectively. And the separation between two end-facets is determined by $\Delta\theta$. (b) The field pattern of resonance at $\lambda = 527\,\text{nm}$. Here $\Delta\theta = 5^\circ$ and the Azimuthal number m is 19. (c) The Q factor and resonant wavelength of different resonances. (d)–(g) are the Q factor, resonant wavelength, effective mode volume, and Purcell effect of the mode with $m = 19$ as a function of $\Delta\theta$.

Q factor. As depicted in Fig. 4(a), a nanowire can be tailored to a ring resonator via nano-manipulation [11]. Fig. 4(b) shows an example of the resonance in the nanowire-based ring-resonator. While the gap introduces some additional loss, the calculated Q factor is still about 100, which is more than an order of magnitude higher than the Fabry-Perot cavity [17]. One may argue that the Q factor of this ring resonator is not as good as regular ring resonator with similar size [20]. Here we will emphasize again the significant advantages of hybrid plasmonic device, the extremely small mode volume (V_{eff}) and larger Purcell factor (F_p). For the mode in Fig. 4(b), the calculated V_{eff} is about $3\times10^{-3}\,\mu\text{m}^3$. Then the corresponding Purcell factor ($Fp = 3Q(\lambda/n)^3/4\pi^2V_{eff}$) can be as high as 90. Both V_{eff} and F_p are orders of magnitude higher than regular dielectric cavity [20, 21], indicating the potential applications in nanosensors and nano-cavity quantum electrodynamics.

The resonance in Fig. 4(b) is not a special mode that generate high Q factor like the modes around avoided resonance crossing [22]. This calculated WG-like modes with different Azimuthal number in Fig. 4(c) shows that the high Q resonance is quite general in the nanowire based ring-resonator. Similar to Fig. 2, the high Q factor is also robust to the changes on separation gap. Figs. 4(d)–(g) show the dependences of quality factor, resonant wavelength, effective mode volume, and Purcell factor on the size of separation distance $\Delta\theta$. With the increase of $\Delta\theta$ (size of air gap), the resonant wavelength shifts to blue side in Fig. 4(e). According to Figs. 2 and 3, the collection ratio of the nanowire also decreases, generating a reduction in Q factor in Fig. 4(d). When $\Delta\theta$ is smaller than 5 degree, which corresponds to a gap size $\Delta\theta \times R$ about 87 nm, the reduction is very slow and the Q factor is very close to that of a perfect ring resonator with $\Delta\theta = 0$. The reduction increases at larger $\Delta\theta$. But the Q factor at $\Delta\theta = 13$ degree (gap size ~ 226 nm) is still around half of the value of perfect ring.

It is important to note that perfect hybrid plasmonic ring-resonator has been thoroughly studied before. In previous studies, the transverse cross-sections are usually the rectangles [23, 24], which is supposed to be fabricated with top-down etching. However, the nanoscale devices are extremely difficult to be fabricated even with E-beam lithography. And the etching faces sever challenge in wide bandgap materials such as GaN, where the surface roughness is too large to kill the light confinement [25].

In Summary, we have studied the photon hopping effect between two nanowires. Based on the high collection ratio at the nanoscale, we proposed a new design to achieve high Q, small V_{eff}, and large F_p simultaneously by tailoring the well-known semiconductor nanowire to a ring-like resonator. As both the synthesis of nanowire and the nanoscale manipulation have been widely explored, our findings will significantly expanding the applications of nanowires in active devices such as nanolasers and passive devices such as nano-waveguide and nano-network.

ACKNOWLEDGMENT

This work is supports by NSFC11204055, SFC61222507, NSFC11374078, NCET-11-0809, KQCX2012080709143322, and KQCX20130627094615410.

REFERENCES

1. Shacham, A., K. Bergmann, and L. P. Caloni, *IEEE Trans. Comput.*, Vol. 57, 1246, 2008.
2. Michalet, X., et al., *Science*, Vol. 307, 538, 2005.
3. Novotny, L., *Nature*, Vol. 455, 887, 2008.
4. Yan, R. X., D. Gargas, and P. D. Yang, *Nature Photon.*, Vol. 3, 569, 2009.
5. Xia, Y., et al., *Adv. Mater.*, Vol. 15, 353, 2003.
6. Huang, M. H., et al., *Science*, Vol. 292, 1897, 2001.
7. Zapien, J. A., et al., *Appl. Phys. Lett.*, Vol. 84, 1189, 2004.
8. Duan, X., Y. Huang, R. Agarwal, and C. M. Lieber, *Nature*, Vol. 421, 241, 2003.
9. Johnson, J. C., et al., *Nature Mater.*, Vol. 1, 106, 2002.
10. Chin, A. H., et al., *Appl. Phys. Lett.*, Vol. 88, 163115, 2006.
11. Pauzauskie, P. J., D. J. Sirbuly, and P. D. Yang, *Phys. Rev. Lett.*, Vol. 96, 143903, 2006.
12. Qian, F., et al., *Nature Mater.*, Vol. 7, 701, 2008.
13. Li, Y., F. Qian, J. Xiang, and C. M. Lieber, *Mater. Today*, Vol. 9, 18, 2006.
14. Barnes, W. L., A. Dereus, and W. Ebbesen, *Nature*, Vol. 424, 824, 2003.
15. Ditlbacher, H., et al., *Phys. Rev. Lett.*, Vol. 95, 257403, 2005.
16. Oulton, R. F., V. J. Sorger, D. A. Genov, D. F. P. Pile, and X. Zhang, *Nature Photon.*, Vol. 2, 496, 2008.
17. Oulton, R. F., et al., *Nature*, Vol. 461, 629, 2009.
18. Yu, Y.-J., et al., *Science*, Vol. 337, 450, 2012.
19. Seidel, J., S. Grafstrom, L. Eng, and L. Bischoff, *Appl. Phys. Lett.*, Vol. 82, 1368, 2003.
20. Song, Q. H., H. Cao, S. T. Ho, and G. S. Solomon, *Appl. Phys. Lett.*, Vol. 94, 061109, 2009.
21. Song, Q. H. and H. Cao, *Phys. Rev. Lett.*, Vol. 105, 053902, 2010.
22. Song, Q. H., Z. Y. Gu, S. Liu, and S. M. Xiao, *Sci Rep.*, Vol. 4, 4858, 2014.
23. Xiao, Y.-F., et al., *J. Phys. B: Atomic, Molecular and Optical Physics*, Vol. 43, 035402, 2010.
24. Chen, Y., C. Zou, Y. Hu, and Q. Gong, *Phys. Rev. A*, Vol. 87, 023824, 2013.
25. Zhang, Y., et al., *Phys. Status. Solidi.*, Vol. 247, 1713, 2010.